Transactions of the Materials Research Society of Japan 26 [3] 963-966 (2001)

Roles of Electron Correlation and Orbital Degree of Freedom in Manganese Oxides

Sumio Ishihara, Satoshi Okamoto and Sadamichi Maekawa

Institute for Materials Research, Tohoku University,
Sendai 980-8577, JAPAN
Fax: 81-22-215-2006, e-mail: ishiha@imr.tohoku.ac.jp

Roles of electron correlation and orbital degree of freedom in manganese oxides with perovskite structure are theoretically investigated. In particular, correlation between orbital structure and maganetic ordering in double layered manganites is examined. It is shown that the relative stability of the two e_g orbitals, i.e. $d(3z^2\text{-}r^2)$ and $d(x^2\text{-}y^2)$ orbitals in a Mn ion, dominates the magnetic ordering. We explain a mechanism of the correlation between orbital and magnetism by a microscopic theory with strong electron correlation.

Key words: perovskite manganites, orbital degree of fredom, electron correlation

1. INTRODUCTION

Perovskite manganites $A_{1-x}B_xMnO_3$ (A=La, Pr, Nd, Sm, B=Ca, Sr, Ba) and their related compounds have recently received much attention because of a lot of fruitful and dramatic phenomena such as the colossal magnetoresistance (CMR) [1]. It is well recognized that the manganites are the typical compounds where spin, charge and orbital degrees of freedom as well as lattice are strongly coupled with each other. The electron configuration of a Mn^{3+} ion is $(3d)^4$. Due to the crystalline field with the cubic symmetry, the degenerate five $3d$ orbitals split into the doubly degenerate e_g orbitals and the triply degenerate t_{2g} ones. Since the intra-atomic Hund coupling is stronger than this energy splitting, one electron occupies one of the two e_g orbitals. Therefore, this ion has orbital degree of freedom as well as spin and charge ones. This degree of freedom shows a long range ordering, i.e. the orbital ordering, as does the spin degree of freedom. Several types of the orbital ordered phases are suggested theoretically and experimentally. It is recognized that these orderings control the magnetic, optical and transport properties

Manganites with layered crystal structure $A_{2-2x}B_{1+2x}Mn_2O_7$ are another class of CMR materials [2-7]. In this crystal structure, pairs of the MnO_2 layers are stacked along the c axis. The reduced dimensionality in this crystal not only causes the strong anisotropy in the electrical resistivity but also enhances a magnitude of CMR near the ferromagnetic transition temperature. It is experimentally revealed that with doping of holes, the magnetic structure changes as AFM-II ($0.29<x<0.31$), FM ($0.31<x<0.39$), FM+AFM-I ($0.39<x<0.48$) and AFM-I ($0.48<x<0.49$) [7]. Here, FM and AFM indicate ferromagnetic and antiferromagnetic structures, respectively. In AFM-I(II) structure, spins are ferromagnetically aligned in the ab plane, antiferromagnetically (ferromagnetically) in the c axis within a bilayer, and ferromagnetically (antiferromagnetically) between the nearest neighboring bilayers. At the same time, the lattice structure changes systematically with changing carrier concentration; with doping of holes, a Mn-O bond length in a MnO_6 octahedron is gradually elongated (shorten) in the ab plane (c axis) [4,6,7]. These results strongly suggest that the orbital character of the e_g electrons is also systematically changed with carrier concentration and controls the magnetic ordering in layered manganites.

In this paper, we examine correlation between magnetic ordering and orbital structure in layered manganites. The level separation between the two e_g orbitals is estimated in the ionic model for a large number of the compounds. It is found that a universal correlation between the relative stability of orbitals and the magnetic transition temperatures. We explain a mechanism of this correlation by a theory based on the model where the two e_g orbital and strong electron correlation are taken into account.

2. CORRELATION BETWEEN ORBITAL AND MAGNETISM IN LAYERED MANGANITES

We examine correlation between several physical parameters obtained from the structural data in a number of samples and their magnetic transition temperatures. Since the intra-bilayer magnetic coupling is much larger than the inter-bilayer one, we term the AFM-I structure the A-type AFM one and regard the AFM-II as the FM. The structural data utilized here were obtained from the neutron and x-ray scattering experiments in Refs. 7-18. In manganites with pseudo-cubic perovskite structure, it is well known that the tolerance factor is one of the good parameters to arrange the magnetic transition temperatures [19]. This is because this factor controls the Mn-O-Mn bond angle which governs the magnitude of the ferromagnetic interaction in the double exchange scenario. In layered manganites, we define the tolerance factor as

$$t = \frac{d(O-A)}{\sqrt{2}d(Mn-O)} \quad , \qquad (1)$$

where $d(O\text{-}A)$ and $d(Mn\text{-}O)$ are the averaged bond lengths between nearest neighboring O-$A(B)$ and Mn-O ions in the ab plane, respectively. We plot the FM transition temperature T_C and the Neel temperature T_N for the A-type AFM structure for a number of samples as functions of the tolerance factor. It is shown that tolerance factor is located around t=1 and the transition temperatures are distributed randomly in a narrow region of t. Correlation between a Mn-Mn bond length d(Mn-Mn) and the magnetic transition temperatures are also examined. We find that T_C is not correlated with d(Mn-Mn) and that T_N increases with increasing d(Mn-Mn). However, this tendency of T_N is opposite to the prediction of the conventional double exchange scenario, where the ferromagnetic interaction decreases with increasing the Mn-Mn bond length. We also examined correlations between $T_{C(N)}$ and a Mn-O-Mn bond angle in the c axis, a lattice spacing between the bilayers and lattice constants. However, there are not clear correlation between these parameters and the transition temperatures.

Now we consider the correlation between magnetic ordering and orbital structure. To examine the level splitting for the two e_g orbitals, the ionic model is adopted. This model may be justified by the following considerations[20,21,22]: (1) $LaMnO_3$ is an ionic insulator where the ionic model provides a good starting point for the electronic structure. (2) The ionic properties are predominant between bilayers. (3) The energy level structure based on the model, where the covalency effects between Mn and O ions are taken into account, shows the same tendency with those by the ionic model. This is because the two orbitals with the e_g symmetry considered here are the so-called anti-bonding orbitals constructed by the Mn $3d$ and O $2p$ orbitals. The Madelung potential for a hole in the $d(3z^2\text{-}r^2)$ and $d(x^2\text{-}y^2)$ orbitals at site j are defined as

$$V(3z^2-r^2) = \frac{1}{2}\left\{V(\vec{r}_j + r_d\hat{z}) + V(\vec{r}_j - r_d\hat{z})\right\} \quad , \qquad (2)$$

and

$$V(x^2-y^2) = V(\vec{r}_j + r_d\hat{x}) \quad , \qquad (3)$$

respectively. Here $V(r_j)$ is given by

$$V(\vec{r}_j) = \sum_{i\neq j}\frac{Z_i e^2}{|\vec{r}_i - \vec{r}_j|} \quad , \qquad (4)$$

with a point charge $Z_i e$ at site i and the position r_i . r_d (=0.42 Å)is the radius of a Mn $3d$ orbital where its radial density is maximum. To calculate Eq. (4), the Ewald method is utilized. We choose Z_i's for Mn, O and A ions are 3+x, -2 and (8-2x)/3, respectively. The

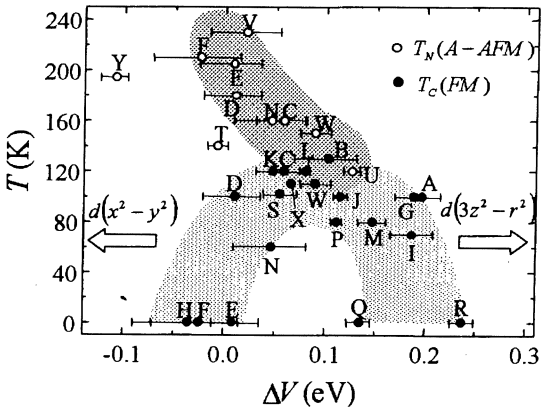

Fig. 1: The Curie temperatures (T_C) for the FM structure and the Neel temperatures (T_N) for the A-type AFM structure as functions of ΔV. Filled and open circles indicate T_C and T_N , respectively. ΔV's are evaluated for the following compounds: A: $La_{1.4}Sr_{1.6}Mn_2O_7$ [7], B: $La_{1.3}Sr_{1.7}Mn_2O_7$ [7], C: $La_{1.2}Sr_{1.8}Mn_2O_7$ [7], D: $La_{1.1}Sr_{1.9}Mn_2O_7$ [7], E: $La_{1.04}Sr_{1.96}Mn_2O_7$ [7], F: $LaSr_2Mn_2O_7$ [7], G: $La_{1.4}Sr_{1.6}Mn_2O_7$ [8], H: $Pr_{1.4}Ca_{1.6}Ba_{0.3}Mn_2O_7$ [9], I: $Nd_{1.4}Ca_{1.6}Mn_2O_7$ [10], J: $La_{1.4}Sr_{1.6}Mn_2O_7$ [11], K: $La_{1.2}Sr_{1.8}Mn_2O_7$ [12], L: $La_{1.2}Sr_{1.8}Mn_2O_7$ [13], M: $La_{1.2}(Sr_{0.8}Ca_{0.2})_{1.8}Mn_2O_7$ [13], N: $La_{1.4}(Sr_{0.7}Ca_{0.3})_{1.8}Mn_2O_7$ [13], O: $La_{1.4}(Sr_{0.6}Ca_{0.4})_{1.8}Mn_2O_7$ [13], P: $(La_{0.8}Nd_{0.2})_{1.2}Sr_{1.8}Mn_2O_7$ [13], Q: $(La_{0.6}Nd_{0.4})_{1.2}Sr_{1.6}Mn_2O_7$ [13], R: $Sm_{1.2}Sr_{1.8}Mn_2O_7$ [14], S: $La_{1.4}Sr_{1.4}Ca_{0.4}Mn_2O_7$ [15], T: $NdSr_2Mn_2O_7$ [16], U: $Nd_{1.1}Sr_{1.9}Mn_2O_7$ [16], V: $LaSr_2Mn_2O_7$ [17], W: $LaSr_{1.6}Ca_{0.4}Mn_2O_7$ [18], X: $NdSr_2Mn_2O_7$ [18]. In the region with large positive (negative) value of ΔV, the $d(3z^2\text{-}r^2)$ ($d(x^2\text{-}y^2)$) orbital is occupied by an electron.

difference between the potentials defined as

$$\Delta V = V(3z^2-r^2) - V(x^2-y^2) \quad , \qquad (5)$$

represents the relative stability of the two e_g orbitals.

The magnetic transition temperatures for a number of layered compounds are plotted as functions of ΔV (Fig.1). It is clearly shown that there is correlation between the magnetic transition temperatures and ΔV; T_N's for the A-type AFM structure increase with decreasing ΔV and T_C 's for the FM structure have a maximum at around $\Delta V \sim 0.083$eV . These results imply that the stability of the A-type AFM structure is correlated with that of the $d(x^2\text{-}y^2)$ orbital and there exists the optimal orbital structure for the FM ordering.

In Fig. 2, The magnetic phase diagram at T=0 is plotted as a function of ΔV. It is shown that the magnetic structure at T=0 is governed by ΔV and x; the FM phase is located in the region with smaller x and moderate ΔV and the A-type AFM phase is with larger x and smaller ΔV.

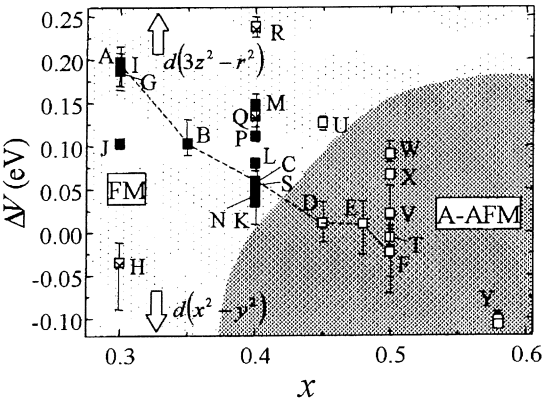

Fig. 2: The magnetic phase diagram at $T=0$ as a function of ΔV and x. Filled, open and crossed squares indicate the FM, A-type AFM, and paramagnetic samples, respectively. ΔV's are calculated for the same samples in Fig. 1. In the region with large positive (negative) value of ΔV, the $d(3z^2\text{-}r^2)$ ($d(x^2\text{-}y^2)$) orbital is occupied by an electron. The dotted lines indicate a series of to $La_{2-2x}Sr_{1+2x}Mn_2O_7$.

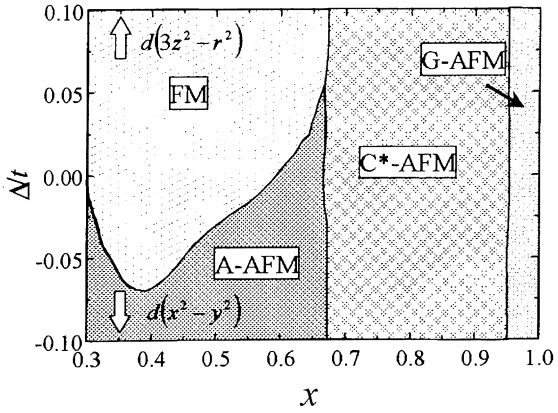

Fig. 3: The calculated magnetic phase diagram at $T=0$ as a function of Δ and x. Δ is the splitting of the energy level between the $d(3z^2\text{-}r^2)$ and $d(x^2\text{-}y^2)$ orbitals. Δ corresponds to $\Delta V/\varepsilon(\infty)$ where the dielectric constant $\varepsilon(\infty)$ is about 3-3.5 in manganites. In the region with large positive (negative) value of Δ, the $d(3z^2\text{-}r^2)$ ($d(x^2\text{-}y^2)$) orbital is occupied by an electron.

3. MECHANISM OF THE CORRELATION

Let us examine a mechanism of the correlation between orbital structure and the magnetic transitions based on a microscopic theory. We start with the tight-binding Hamiltonian. Here we consider a pair of the two dimensional sheets of a squared lattice consisting of Mn ions. In each Mn ion, the two e_g orbitals are introduced and the t_{2g} electrons are treated as a localized spin. Because of the strong intra-site Coulomb interactions in a Mn ion, the doubly occupied states of electrons are prohibited at a Mn site. Then, we derive the following effective model Hamiltonian describing the low energy electronic states by the perturbational procedure [22,23]:

$$H = H_t + H_J + H_H + H_{AF} + H_\Delta \quad , \quad (6)$$

with

$$H_t = \sum_{<ij>\gamma\gamma'\sigma} t_{ij}^{\gamma\gamma'} d_{i\gamma\sigma}^{+} d_{j\gamma'\sigma} + H.c. \quad , \quad (7)$$

$$H_J = -2\sum_{<ij>} J_1 \left(\frac{3}{4} n_i n_j + \vec{S}_i \cdot \vec{S}_i\right)\left(\frac{1}{4} - \tau_i^l \tau_j^l\right) - 2\sum_{<ij>} J_2 \left(\frac{1}{4} n_i n_j - \vec{S}_i \cdot \vec{S}_i\right)\left(\frac{3}{4} + \tau_i^l \tau_j^l + \tau_i^l + \tau_j^l\right) \quad , \quad (8)$$

$$H_H + H_{AF} = -J_H \sum_i \vec{S}_i \cdot \vec{S}_{ti} + \sum_{<ij>} J_{AF} \vec{S}_{ij} \cdot \vec{S}_{ti} \quad , \quad (9)$$

and

$$H_\Delta = -\Delta \sum_i T_{iz} \quad . \quad (10)$$

$d_{i\sigma\gamma}$ is the annihilation operator for an e_g electron with spin σ and orbital γ at site i. This operator excludes the doubly occupied states of electrons due to the strong electron correlation. S_i is the spin operator for e_g electron with $S=1/2$ and S_{ti} is that for t_{2g} electrons with $S=3/2$. T_i is a pseudo-spin operator for orbital degree of freedom defined by

$$\vec{T}_i = \frac{1}{2} \sum_{\gamma\gamma'\sigma} d_{i\gamma\sigma}^{+} \vec{\sigma}_{\gamma\gamma'} d_{i\gamma'\sigma} \quad , \quad (11)$$

where σ_μ is the Pauli matrices with $\mu=(x,y,z)$ and $\tau_i^l = \cos(2\pi m_l/3) T_{iz} - \sin(2\pi m_l/3) T_{ix}$ with $(m_x, m_y, m_z)=(1, 2, 3)$. l indicates the direction of a bond connecting site i and site j. The up and down pseudo-spin states describe the states where the $d(3z^2\text{-}r^2)$ and $d(x^2\text{-}y^2)$ orbitals are occupied by an electron, respectively. H_t and H_J correspond to the so-called t and J terms in the t-J model for High-Tc cuprates, respectively. However, unlike the conventional t-J model, the orbital degree of freedom is taken into account in these terms. $t^{\gamma\gamma'}_{ij}$ is the hopping integral between the nearest neighboring Mn ions, and $J_1=t^2/(U'\text{-}I)$ and $J_2=t^2/U$ are the exchange interactions between the e_g electrons where U, U' and I are the intra-orbital Coulomb interaction, the inter-orbital one and the exchange interaction, respectively. t is the hopping integral between the nearest neighboring $d(3z^2\text{-}r^2)$ orbitals along the c axis and is about 0.5-0.7eV. H_H and H_{AF} represent the Hund coupling (J_H)

between e_g and t_{2g} spins, and the antiferromagnetic superexchange interactions (J_{AF}) between the nearest neighboring t_{2g} spins, respectively. The last term in Eq. (6) represents the splitting of the energy level (Δ) between the $d(3z^2\text{-}r^2)$ and $d(x^2\text{-}y^2)$ orbitals at a Mn site. Δ corresponds to $\Delta V/\varepsilon(\infty)$ introduced in the previous section where the dielectric constant $\varepsilon(\infty)$ is about 3-3.5 in manganites. In order to obtain the magnetic phase diagram based on this model Hamiltonian, we adopt the mean field approximation in the slave-boson scheme. Here, the operator $d_{i\gamma\sigma}$ in Eq. (7) is decomposed as

$$d_{i\gamma\sigma} = f_i^{+}\tau_{i\gamma}s_{i\sigma} \quad , \quad (12)$$

where f_i and $s_{i\sigma}$ are bosonic operators for charge and spin degrees of freedom, respectively, and $\tau_{i\gamma}$ is a fermionic one for orbital degree of freedom. The constraints for these operators are treated as a mean field sense. Because the hole concentration is larger than 30% in the region of the present interest, H_J in Eq. (6) is supposed to be irrelevant and neglected in the calculation. A detailed calculation method will be presented elsewhere. The phase diagram for manganites with bilayred structure has also been studied in the Hartree-Fock theory in Ref. 24.

The calculated results of the magnetic phase diagram at $T=0$ is presented in Fig. 3. The parameter values are chosen to be J_{AF}/t=0.025. It is shown that the characteristic features shown in Fig. 3 are well reproduced by the present theoretical results in the regions of $0.3<x<0.6$; the A-type AFM phase appears in the region with higher x and smaller Δ than that of the FM one. The calculated results show that, in the A-type AFM phase, the orbital character is almost of the $d(x^2\text{-}y^2)$-type. On the other hand, in the FM phase, the character of the occupied orbital shows a mixture of the $d(3z^2\text{-}r^2)$ and $d(x^2\text{-}y^2)$ orbitals. The present results suggest that a dimensionality of the FM interaction is controlled by orbital structure; in the A-type AFM structure, the FM interaction in the *ab* plane is caused by the double exchange interaction, while the AFM interaction in the *c* direction is by the AFM superexchange interaction. When the $d(x^2\text{-}y^2)$ orbital is stabilized, the double exchange interaction in the *ab* plane (*c* direction) becomes strong (weak) and the A-type AFM structure is stabilized. A moderate mixing of the orbitals is indispensable to realized the FM phase where the double exchange interaction overcomes the AFM superexchange interaction in the three directions. In Fig. 3, the C* and G-type AFM phases appear in the region of the higher hole concentration. Spins are ferromagnetically aligned in the *b* axis and antiferromagnetically in the *a* and *c* axes in the C*-type AFM phase, and are antiferromagnetically aligned in the three directions in the G-type AFM phase. The C* and G-type phases are recently confirmed by the neutron scattering experiments in $La_{2-2x}Sr_{1+2x}Mn_2O_7$ with $0.74<x<0.9$ and $0.9<x<1.0$, respectively [18]. It is supposed from the measured crystal structure that the occupied orbitals have a $d(3y^2\text{-}r^2)$ character in the C*-type AFM state. This is also consistent with the present calculated results.

ACKNOWLEDGEMENTS

The authors would like to thank Y. Moritomo, Y. Tokura, T. Kimura, Y. Endoh, K. Hirota, and J. F. Mitchell for their valuable discussions. This work was supported by Science and Technology Special Coordination Fund for Promoting Science and Technology, CREST, New Energy and Industrial Technology Development Organization (NEDO) and Grant-in-Aid for Scientific Research Priority Area from the Ministry of Education, Science and Culture of Japan. S. O. acknowledges the financial support of JSPS. Part of the numerical calculation was performed in the HITACS-3800/380 superconputing facilities in IMR, Tohoku Univ.

4. REFERENCES

[1] For a review see "Colossal Magnetoresisitance Oxides" Ed. by Y. Tokura, Gordon and Breach, (2000).

[2] Y. Moritomo *et al.*, *Nature (London)*, **380**, 141-44 (1996).

[3] T. Kimura *et al.*, *Science*, 274, 1698-701 (1996).

[4] M. Medarde *et al.*, *Phys. Rev. Lett.*, **83**, 1223-26 (1999).

[5] Y. Moritomo *et al.*, *Phys. Rev. B*, **56**, R7057-60 (1997).

[6] T. Kimura *et al.*, *Phys. Rev. Lett.*, **81**, 5920-23 (1998).

[7] M. Kubota *et al.*, *J. Phys. Soc. Jpn.*, **69**, 1606-09 (2000).

[8] D. N. Argyriou *et al.*, *Phys. Rev. B*, **59**, 8695-702 (1999).

[9] P. Laffez *et al.*, *J. Appl. Phys.*, **80**, 5850-56 (1996).

[10] E.-O. Chi *et al.*, *Phys. Rev. B*, **60**, 12867-73 (1999).

[11] D. N. Argyriou *et al.*, *Phys. Rev. Lett.*, **78**, 1568-71 (1997).

[12] T. Akimoto *et al.*, *Phys. Rev. B*, **59**, R14153-56 (1999).

[13] P. D. Battle *et al.*, *J. Appl. Phys.*, **83**, 6379-84 (1998).

[14] C. H. Shen *et al.*, *J. Appl. Phys.*, **86**, 2178-84 (1999).

[15] P. D. Battle *et al.*, *Phys. Rev. B*, **54**, 15967-77 (1996).

[16] R. Seshadri *et al.*, *Solid State Commun.*, **101**, 453-457 (1997).

[17] T. Akimoto *et al.*, *Phys. Rev. B*, **61**, 11270-73 (2000).

[18] C. D. Ling *et al.*, (unpublished) *cond-mat/0007253*.

[19] H. Y. Hwang *et al.*, *Phys. Rev. Lett.*, **75**, 914-17 (1995).

[20] Y. Ohta, *et al. Phys. Rev. B*, **43**, 2968-82 (1991).

[21] S. Ishihara, *et al. J. Phys. Soc. Jpn.*, **66**, 2965-68 (1997).

[22] S. Okamoto, *et al.*, *Phys. Rev. B*, **63**, (2001) (to be published).

[23] S. Ishihara, *et al. Physica C*, **263**, 130-33 (1996), and *Phys. Rev. B*, **55**, 8280-86 (1997).

[24] R. Maezono and N. Nagaosa, *Phys. Rev. B*, **61**, 1825-30 (2000).

(Received December 8, 2000; Accepted January 4, 2001)